Language Models in Software Development Tasks: An Experimental Analysis of Energy and Accuracy

Negar Alizadeh*, Boris Belchev[†], Nishant Saurabh*

*Utrecht University, Utrecht, The Netherlands
{n.s.alizadeh, n.saurabh}@uu.nl

[†]University of Twente, Enschede, The Netherlands
b.belchev@student.utwente.nl

Patricia Kelbert[‡], Fernando Castor[†]

[‡]Fraunhofer IESE, Kaiserslautern, Germany
patricia.kelbert@iese.fraunhofer.de

[†]University of Twente, Enschede, The Netherlands
f.castor@utwente.nl

Abstract—The use of generative AI-based coding assistants like ChatGPT and Github Copilot is a reality in contemporary software development. Many of these tools are provided as remote APIs. Using third-party APIs raises data privacy and security concerns for client companies, which motivates the use of locallydeployed language models. In this study, we explore the tradeoff between model accuracy and energy consumption, aiming to provide valuable insights to help developers make informed decisions when selecting a language model. We investigate the performance of 18 families of LLMs in typical software development tasks on two real-world infrastructures, a commodity GPU and a powerful AI-specific GPU. Given that deploying LLMs locally requires powerful infrastructure which might not be affordable for everyone, we consider both full-precision and quantized models. Our findings reveal that employing a big LLM with a higher energy budget does not always translate to significantly improved accuracy. Additionally, quantized versions of large models generally offer better efficiency and accuracy compared to full-precision versions of medium-sized ones. Apart from that, not a single model is suitable for all types of software development tasks.

Index Terms—LLMs, Energy Efficiency, Trade-Offs, Software Development, Coding Assistant, Model Quantization

I. INTRODUCTION

Generative Large Language Models (LLMs, or simply "language models") gained widespread availability with the release of ChatGPT at the end of 2022 [1]. According to recent reports [2], the adoption of generative AI nearly doubled in under six months. Code-specific AI models have revolutionized software development as they are particularly beneficial to developers. Notably, 76% of respondents in Stack Overflow's annual survey reported that they currently use or plan to use AI code assistants [3]. According to a GitHub report [4], developers who participated in their trial quickly integrated GitHub Copilot into their daily workflows and found it extremely valuable. This high level of adoption underscores the AI assistant's role as an essential tool that enhances productivity, streamlines the coding process, and increases efficiency by providing real-time debugging assistance and automating routine tasks.

Although third-party services are widely used for these purposes, with ChatGPT and GitHub Copilot being the most popular [3], reliance on third-party APIs raises concerns for many companies regarding security, data privacy, and subscription costs. Thus, there is a growing interest in local

solutions, with many individuals and organizations seeking to set up their own AI coding assistant using open-access, often smaller language models, but still comparable to publicly available alternatives. One approach for deploying LLMs locally is to utilize a flagship GPU with sufficient memory optimized for Deep Learning (DL) applications and to set up an open-access LLM on it. However, since these GPUs are not affordable for everyone, an alternative solution could be using compressed and quantized models that can run on smaller GPUs or even large CPUs. On the other hand, although LLMs simplify many tasks, this convenience comes with significant costs. Their power consumption is a major concern, leading not only to substantial financial expenses but also to high carbon emissions [5], [6]. While we cannot slow down the expansion of DL in daily life, we can raise awareness about its energy consumption and encourage informed decision-making before deploying models.

The competitive drive among AI companies to release everincreasingly capable LLMs has resulted in the development of models that are inevitably both computationally and energyintensive. Previous works have investigated the energy consumption of language models [7], [8].

However, most studies have primarily focused on energy consumption during the training phase, with limited research examining the inference phase, even though inference can contribute significantly to long-term energy usage [8]. Furthermore, recent studies evaluating code-centric LLMs have mainly concentrated on their performance in terms of accuracy, often overlooking their energy footprint [9], [10]. To the best of our knowledge, this study is the first one evaluating a broad range of LLMs specifically employed in various software development tasks.

The goal of this study is to investigate the energy consumption of using LLMs during the inference phase in typical software development tasks, namely code generation, bug fixing, docstring generation, and test case generation. We aim to cover two real-world scenarios: the first utilizes a single GPU specifically designed for data centers and AI applications and the second involves direct access to a commodity, end-user GPU. In particular, we address the

following research questions:

- RQ1 How does the energy consumption of models vary across typical software-related tasks?
- RQ2 How does the performance of different models vary in terms of energy efficiency and accuracy when executing the same task? Is there a trade-off between energy efficiency and accuracy?
- RQ3 Are there specific model characteristics (e.g., feedforward network dimension, number of transformer blocks) that consistently impact energy?
- RQ4 What are the performance differences between general-purpose models and models specifically optimized for code-centric tasks?

In this study, we evaluate a diverse set of LLMs, comprising 18 model families in 3 different precision formats. Our findings indicate that while the energy footprint of the same model varies widely across different software development tasks, its energy usage per generated token remains consistent. Additionally, the total energy consumed by each model is strongly correlated with its architectural characteristics, suggesting that some aspects of an LLM's architecture can help estimate its efficiency, given that the average size of the outputs can be anticipated. Finally, we observed that energy consumption and accuracy do not always require a compromise, as larger models often have a significantly higher energy footprint while performing similarly, or even being outperformed by, smaller models in terms of accuracy. The replication package for this study, along with the appendices, is publicly available [11].

II. LANGUAGE MODELS

Language models are machine learning models based on the transformer [12] architecture whose main task is, given a sequence of tokens, to predict which tokens are more likely to follow. A language model is composed of multiple transformer blocks, each typically consisting of self-attention mechanisms followed by feed-forward neural networks (FNN). They can be categorized into three architectural categories: encoderonly, decoder-only, and encoder-decoder models [10]. Among these, decoder-only models, are optimized for generating text, making them ideal for content creation [13]. Code-specific language models, in particular, are pre-trained on extensive unlabeled code corpora, whereas general-purpose (or "noncoding") models are trained on a mixture of code and text data [10]. In the remainder of this section, we examine some of the main characteristics of a language model and also briefly introduce the concept of quantized models.

Attention heads enable models to process input sequences in parallel. Each attention head can focus on different relationships and patterns in the data.

Embedding Length is the dimensionality of the vector space in which tokens are represented. Each token is mapped to a vector of this length in a way that similar tokens are close to each other in the embedding vector space.

Feed-Forward Length refers to the size of the intermediate layer in the FNN within each transformer block. The feed-

forward length determines the capacity of this part of the network to comprehend complex interactions between tokens. Quantization refers to representing a model's weights or activations in a lower-precision format (e.g., 8-bit integers) instead of the original high-precision floating-point format [14]. Quantized models undergo the process of reducing the bitwidth of their tensors, which results in a decreased memory footprint and lower computational demands while maintaining acceptable accuracy [15]. This makes quantized models especially valuable for deployment in resource-constrained environments, such as mobile devices or embedded systems, where computational power and memory are limited. Quantization methods can be broadly grouped into two main categories, quantization-aware training and post-training quantization. Former integrates the quantization process within the training phase and Latter applies quantization after the model has been trained [14]. In this study, as we focus on the inference of LLMs, we specifically examine post-training quantization. Preliminary evidence [16] suggests that, among the multiple quantization formats, GGUF (GPT-Generated Unified Format) is the most energy-efficient format currently available. Therefore, we utilized GGUF to compare the quantized versions of the models under examination.

III. RELATED WORK

As highlighted by Watson and colleagues [17], since 2017 DL has been used extensively in solving software engineering tasks. Moreover, the continuous evolution of larger, more capable, and computationally intensive DL models has made examining their energy consumption an increasingly important concern. Despite the growing utilization of LLMs in software-related tasks [3], [4], much of the existing research in evaluating their performance has traditionally focused on metrics such as accuracy [18], [19], or task-specific metrics like pass@k for code synthesis [20]–[23] and repair rate for bug fixing [24].

On the other hand, most of the existing work focuses on the energy usage of the training side [8], [25]–[29]. However, once the model is trained, its energy usage for inference can contribute significantly to long-term energy impact. Because the inference is often a repeated and ongoing process, performed every time a user queries the model, potentially millions of times [30]. At Google [8], for example, inference energy accounts for 3/5 of all the energy spent in ML tasks.

In this section, first, we aim to outline the current state of research related to measuring energy usage during the inference phase of DL models. Luccioni et al. [7] estimated the energy and carbon footprint of the BLOOM 176B model aiming to define and connect the different sources of carbon emissions involved in training and deploying. Following this, subsequent research [31] delved explicitly into the deployment phase of the LLaMa model in 3 different sizes on 2 datasets. Their findings show that the complexity of the input dataset can affect the model's performance. They also suggest power capping as an effective tool for reducing inference energy. In another work, Luccioni et al. [32] conducted a study that provides a comprehensive analysis and comparison of

inference energy costs across a wide range of generative systems, including both task-specific and general-purpose models. The work utilized 88 models over 10 tasks and 30 datasets, including image generation, text completion, etc. that task-specific models are more energy efficient than multi-purpose models when performing the same task. Besides, image-related tasks are more energy-intensive than text-only tasks. Lastly, Desislavov et al. [30] analyzed the energy consumption of DNNs during inference for both vision and NLP tasks. Their findings suggest that better results for DNN models are partly due to algorithmic progress, not just increased computing power. Moreover, hardware improvements can play a role in decreasing DNN energy consumption.

The rest of this section delves into studies that focus on the performance of optimization techniques for LLMs, particularly model quantization. Jin et al. [14] evaluated instruction-tuned LLMs and their quantized versions using various quantization strategies across different parameter scales. They tested these models on 7 knowledge/capacity and 3 question-answering benchmarks, focusing on the Qwen model in 7b, 14b and 72b parameters. The study reported performance metrics like accuracy and BLEU but did not consider energy consumption. They noted that quantization reduces memory usage but can slow down inference. Tuggener et al. [33] reviewed 3 different quantization techniques for LlamaV2-7b. Their findings showed that quantization significantly reduces GPU memory usage but can impact text quality. They also briefly discussed the energy usage involved in fine-tuning these models.

Similarly, Rajput and Sharma [16] benchmarked and analyzed the energy efficiency of various quantization techniques.

None of the aforementioned papers examined the energy consumption of LLMs when performing software development tasks. In this paper, we evaluate the energy impact of 18 model families across 4 different tasks on 2 hardware configurations, while also accounting for model accuracy.

IV. METHODOLOGY

In this study, we examine the energy consumption of openaccess LLMs when supporting software development tasks, from generating code and docstrings to testing and fixing bugs. Figure 1 presents a high-level overview of how we conducted this study. This section outlines the language models we analyzed, the experimental setup, and the methodology used to conduct our experiments.

A. Model Selection

We begin our exploration by gathering a list of top LLMs based on the following criteria:

Popularity: Popularity is measured by the number of downloads of the model sourced from HuggingFace [34]. This will ensure that the results apply to the most commonly used models in real-world scenarios. All GGUF versions of the models were downloaded from Ollama's library [35]. Only pages that explicitly referenced the model's original creators' pages were included, excluding those modified by third parties.

Reputability of creator: While this criterion can be arguably subjective it is still crucial. Companies and research teams that have substantial funding and support from other entities in the field are more likely to develop further and support their models. They are assumed to have a larger infrastructure and more research capabilities as they strive for competitiveness with other key players in the field. Choosing models according to this criterion increases the value of the results as small or medium-sized companies would be more interested in deploying their models.

Availability: Models that are not publicly available for downloading and setting up locally are automatically excluded from this study, such as GPT-3 and GPT-4.

On the other hand, since only GGUF models are supported by Ollama, models must be compatible with conversion to the GGUF format [36]. For example, the Phi3:7b architecture was not supported and could not be included. After failing to find it in the Ollama library, we attempted to convert the original model to GGUF using llama.cpp library [37] but encountered an *Unknown architecture* error.

As this research focuses on integrating LLMs in software development, we have limited our scope to include both general-purpose (non-coding) models and those fine-tuned for code (coding models). We chose instruction-tuned models (additionally trained and polished to understand instructions) over base models because, as shown by the leaderboard [38] maintained by [39], instruction-tuned models consistently outperformed their base counterparts in terms of accuracy. Due to hardware limitations, we also narrowed down our selections to models with no more than 20 billion parameters. The memory constraints of our desktop GPU only allow for quantization levels up to 5 bits. However, [14] shows that reducing the bitwidth below 3 or 2 significantly degrades model performance. Therefore, we limited our quantized collection to 4 and 5 bitwidth for medium-size models (6-8B parameter), and 8 bitwidth for small models (2-4B parameter).

We collected all full-precision, i.e., non-quantized, models and their quantized versions in GGUF format from the Ollama library, preserving the original naming convention. Each model name includes the model family and its parameter size; for example, codellama:13b represents the CodeLLaMA model with 13 billion parameters. The suffixes indicate the precision or quantization level used: fp16 denotes full-precision 16-bit floating-point representation, and -q followed by a number specifies the quantized bit width (e.g., q8 represents an 8-bit quantized version of the model).

B. Hardware, Frameworks, and Libraries

Table I presents a summary of the configuration of the two machines employed in this study. We identify each machine in terms of its GPU. Resource-demanding experiments, including full-precision models and their quantized counterparts, were conducted on a machine equipped with an NVIDIA A100 with 80GB memory, accessed via SSH. The jobs were managed using a job scheduling system (Slurm), as the machine is part of a cluster. On the other hand, experiments with small

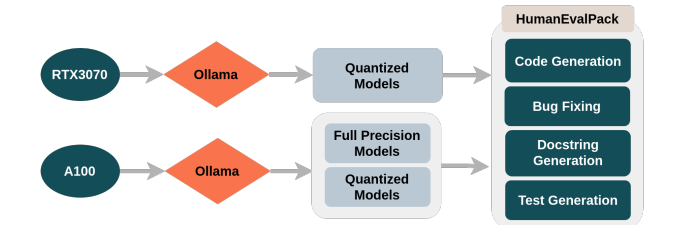


Fig. 1: Schematic representation of the study. The circles represent the models of the NVIDIA GPUs available on the two machines where the experiments were run. The experiments involved quantized and full-precision models. We measured the energy footprint of these models when performing four different tasks, using the workload provided by the HumanEvalPack benchmark.

quantized models were performed on a laptop equipped with an NVIDIA GeForce RTX 3070 GPU. To ensure that all the experiments are running on an isolated GPU, on the cluster system, we pass the *exclusive* flag to the job scheduling system, and on the laptop, we stopped GUI and switched to command-line mode. Each experiment was run three times to reduce the impact of transient variations. The average of all recorded values was reported.

TABLE I: Hardware setup

| DTV 2070 | CPU: Intel Core i7-11850H - 2.5GHz — Mem: 31GB — Cache: |
|----------|--|
| RTX 3070 | 24MB — Governer: Powersave |
| | GPU: NVIDIA GeForce RTX3070 — Mem: 8GB — Power- |
| | Mizer: Adaptive — TGP: 220W |
| | OS: Ubuntu 20.04 (64-bit) |
| | CPU: 2 × AMD 7313 - 3GHz — Mem: 1TB — Cache: 32MB |
| A100 | — Governer: Performance |
| | GPU: NVIDIA A100 PCIe — Mem: 80GB — PowerMizer: High |
| | Performance |
| | OS: AlmaLinux 8.10 (64-bit) |
| | |

Running an LLM locally requires a compatible runtime framework that can handle the model's execution (inference) on various devices. This ensures the model performs efficiently whether it's deployed on desktops, laptops, or another environment. For quantized models in the GGUF format, several open-source frameworks have emerged, including PrivateGPT, Ollama, GPT4All, and llamafile [40]. Among these options, we decided to use the most popular one at the moment, Ollama (v. 0.3.2), based on its number of stars on GitHub, and the ease with which it enables us to switch between models.

For measuring energy and utilization of GPU as in previous studies [41]–[43], we employed the Python binding of the NVIDIA Management Library [44] (pyNVML [45]) to record the GPU power. The profiling rate is set to 10Hz (one sample every 100ms) to avoid the observed overhead for higher rates [43]. The energy usage is then determined as the product of time and average power. As for the energy consumption of the CPU we used a Python library designed for interacting with Intel's RAPL [46] interface named pyRAPL [47]. To

measure the energy usage of the hardware and operating system when idle, we utilized pyRAPL in the Ubuntu terminal, while only the basic operating system services were running on the machine. The sampling rate was 1Hz [48] with a total of 3400 observations collected,

ensuring a 98% confidence level that the real power value lies within $\pm 2\%$ of the observed values. The mean power draw of the CPU in idle mode was 1.92W. Similarly, for measuring the idle power of GPUs we executed the nvidia-smi [49] command for 340 seconds to collect 3400 samples at 100ms intervals. The exact command can be found in the online appendix [11].

The recorded idle power values for RTX3070 and A100 were 9.92W and 46.82W, respectively.

C. Dataset

In studies assessing the coding proficiency of LLMs, HumanEval [21] is the most widely-used benchmark [20]–[23], [50], [51] and has become the de facto standard for this purpose [10]. It consists of 164 hand-written Python programming problems and each problem comes with its own set of test cases. In this study, we employed an extended version of HumanEval called HumanEvalPack [20].

It includes more rigorous test cases and encompasses all of our desired coding tasks: Code Repair (Bug Fixing), Code Explanation (Generating Docstring), Code Synthesis (Generating Code), and Test Assertion Generation covering six programming languages. We evaluate all models on the Python subset of HumanEvalPack. To ensure that each problem, across all four tasks, is accompanied by an explicit example of input-output pairs in the correct format, we added two new columns, one containing a sample test case assertion and the other an example input-output pair for a docstring. These examples were primarily extracted from the provided fields, with a few cases manually added, and are used in the prompt as the function start for the respective task (Appendix A [11]).

D. Experimental Procedure

Hyperparameters. In our preliminary experiments, we observed that hyperparameter changes can impact energy consumption. To eliminate other confounds, we fixed the hyperparameters for all experiments. Following recommendations from prior studies [20], [22], [23], [31], [50] which employed HumanEval as a coding benchmark, we set the top-p value to 0.95 and the temperature to 0.1 across all experiments to ensure a fair comparison. Previous work [21], [22] has shown that increasing the temperature adversely affects the pass@1 metric, with 0.1 identified as the optimal value.

Finally, to ensure the reproducibility of our experiments, all the results are generated using a fixed seed number.

Prompts To ensure a fair comparison and consistency with previous studies in which pre-trained code LLMs are evaluated, we did not optimize prompts but used the same format across all models to distinguish question and answer [20], [52], [53]. Each prompt includes both the instruction

and the function start. Since LLMs are trained on a next-token prediction objective, including the function start helps the model complete it directly without searching within the output [20]. For each task, we adjusted the information in the prompts accordingly. An example of the prompts is available in the online Appendix A [11].

Evaluation To assess the correctness of the outputs generated by LLMs, we employed the mean pass@k (mean success rate) evaluation metric, as defined in the Codex evaluation set [21]. It considers a problem solved if any of the k-generated solutions pass all test cases. We focus on pass@1, which shows the probability of the model solving a problem in one try. Specifically, for code generation tasks, the correctness of the generated code is determined by whether it passes or not, all the hand-written test assertions provided in the dataset. If the code satisfies all test assertions, it is counted as a correct answer. We followed a similar approach for evaluating bug-fixing tasks, where the correctness of the fixed code was measured by its ability to pass the corresponding test assertions. To assess the correctness of the LLM-generated test assertions, we also followed a similar approach. However, in this case, we executed the canonical solution alongside the generated test assertions. We classified a test as incorrect if the canonical solution fails to pass the assertions, either due to incorrect assertions or syntax errors [54]. To assess the thoroughness of the generated tests, we combined the canonical solution with the generated test assertions in a Python file and measured coverage using the Python code coverage analysis tool, coverage.py [55]. To evaluate the correctness of the generated docstrings, we used another LLM as a judge to generate code based on the provided docstring. The generated code was then evaluated using the pass@1 metric. We explored three different options for selecting the judge LLM: (1) feeding the generated docstring back into the model that originally generated it [20], (2) selecting the bestperforming publicly-available, locally executable LLM among the models under evaluation, and (3) utilizing one of the best proprietary LLMs available, more specifically GPT-4o-mini. Based on our investigation, to avoid potential bias, we decided to proceed with the third option.

V. RESULTS

In this section we present the findings of this study. For the sake of reporting and analyzing results, throughout the section we treat different quantization levels and numbers of parameters for the same language model family as different models. Models are grouped into families based on the organization developing them, their architecture, and their parameter count. For example, we refer to gemma:2b-q8 and gemma:2b-q4 as different models within the same family. However, gemma:7b-q8 belongs to a different family. This makes sense as they are made available separately, have different memory requirements, and often different architectures. We organize the presentation of the results in terms of our main findings.

A. Models exhibit different energy consumption for different software development tasks and different models vary widely in how they perform the same task.

To compare a model's energy consumption across different tasks, we report the GPU's total energy usage in watt-hours (Wh). Figures 2 and 3 present the energy footprint of the analyzed models in the four tasks, for the two machines. In the remainder of the paper, except where explicitly noted, we focus on the A100 machine. Moreover, in this section, we are only concerned with energy consumption, as the use of these models incurs an energy cost independently of whether they are accurate or not. In Section V-B we also take model accuracy into account.

In Figure 2, bars representing the same language model families, with the same number of parameters, have the same color. The figure shows that different tasks entail different energy use and Test Generation and Bug Fixing are the most energy-intensive tasks. The mean energy consumed across all the models for Code Generation, Docstring Generation, Bug Fixing, and Test Generation was, respectively, 13.46Wh, 19.12Wh, 29.69Wh, and 37.94Wh. Column "Total energy (Wh)" of Table II presents numerical results for the energy consumption of the models, across the tasks. Numerical results for the RTX 3070 are available in the online Appendix B [11].

The difference in the energy consumption of the same model for different tasks can be large. Model llama2:7b-q8 consumed 7.2x more energy for Test Generation than it did for Code Generation, whereas granite-code:20b-fp16 consumed 2.45x more energy for Bug Fixing than it did for Docstring Generation. This is consistent for Test Generation, although the difference is smaller in some cases. For example, Test Generation with gemma:2b-fp16 consumed only 27.6% more energy than Code Generation. There was no scenario where a model consumed more energy for Code Generation than Test Generation. When considering Test Generation and Docstring Generation, the phi3:3.8b family of models was the only one where the latter required more energy than the former (74% more for phi3:3.8b-q8). Comparing Bug Fixing and Test Generation, for 2/3 of the model families the latter required more energy than the former. The difference can be significant, e.g., starcoder2:15b-q8 consumed three times more energy when generating tests, compared to fixing bugs. Conversely, Bug Fixing with granite-code:20b-q8 required 72.19% more energy than Test Generation. Bug Fixing was generally more expensive than Code Generation and Docstring Generation. Only the gemma:2b family exhibited a higher energy footprint for Code Generation than Bug Fixing. In addition, two families of models, starcoder2:15b and codellama:13b, required consistently more energy for Docstring Generation than Bug Fixing and, phi3:14b, exhibited similar results for both tasks. Finally, Code Generation was the task requiring the least energy. Only three model families consumed consistently more energy to generate code than to generate documentation, codegemma:7b, gemma:2b, and deepseek-coder:1.3b, and two had very similar results, gemma:7b and granite-code:3b.

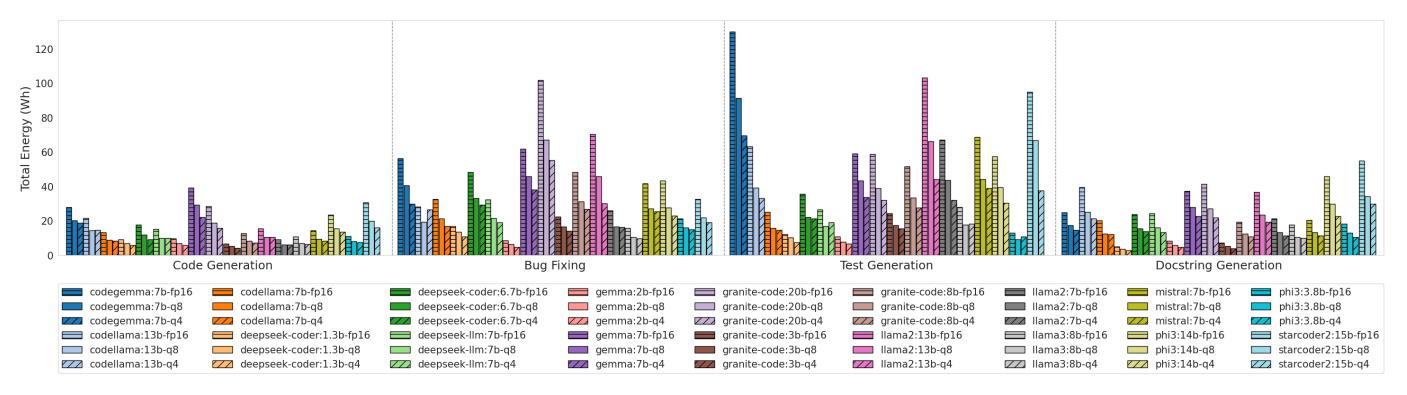


Fig. 2: Energy (Wh) consumed by the A100 GPU when performing each task. Model names are presented according to the pattern family-QQ, where family includes the family name (phi3, gemma, llama3, etc.) and the number of parameters, in billions (20b, 3.8b, etc.), and QQ is the quantization level (4 bit, 8 bit, or full precision 16 bits).

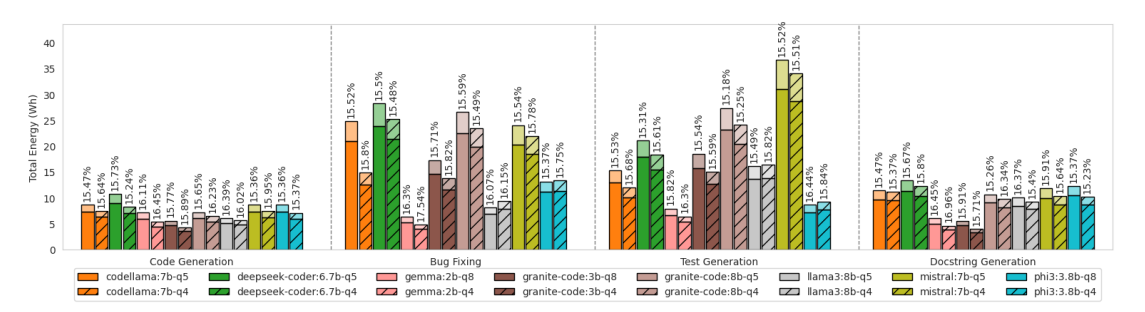


Fig. 3: Energy (Wh) consumed by the RTX 3070 GPU and the Intel Core i7 CPU when performing each task. The lower part of each bar represents GPU energy, and the upper part represents CPU energy. Model names follow the pattern of Figure 2.

Zooming into each task individually also reveals great variation in energy consumption. For example, gemma:7b-fp16 consumed 9.17 times more energy than granite-code:3b-q4 for Code Generation. There is even more variation for the other tasks. The most energy-hungry model in Bug Fixing, granite-code:20b-fp16, consumed almost 21 times more energy than the least energy-hungry, gemma:2b-q4. In a similar vein, the most energy-hungry models for Docstring Generation and Test Generation, starcoder2:15b-fp16 and codegemma:7b-fp16, respectively, consumed 19.68 and 19.12 times more energy than the least consuming ones in the respective tasks, deepseek-coder:1.3b-q4 and gemma:2b-q4. Overall, we have seven different models occupying the extremes for the four tasks. If energy efficiency is an important quality attribute, considering the task at hand is essential.

Figure 2 highlights two trends. First, for the same task, full-precision variants of a model family consistently used more energy than their quantized counterparts. Moreover, 8-bit quantized models exhibited higher energy consumption than their 4-bit counterparts. The few exceptions involved only quantized variants and the differences were relatively small, e.g., 2% for Test Generation with llama3:8b. Figure 3 shows a similar phenomenon. There are a few more exceptions (4 out of 32), but this is expected as the number of quantization bits is similar (5 vs. 4). Second, models with more parameters tend to consume more energy, but only for large differences, relative

to model sizes, e.g., 15b vs. 7b models. When differences are smaller, the number of parameters is not a good predictor for the energy footprint of the models. For example, phi3:14b-fp16 requires 10.33% more energy to generate docstrings than granite-code:20b-fp16, 57.33% less to fix bugs, and the two models are virtually tied in Test Generation.

It is important to note that even different variants of the same model are not always comparable. For example, in Figure 2, although Codellama:13b-q8 and Codellama:7b-fp16 are close in size (14GB vs. 13GB), with the former having twice as many parameters at 8-bit precision and the latter having half as many parameters at full precision, their energy footprint differs. They show similar energy usage for code generation, but this does not hold for other tasks due to differences in their characteristics. This topic is explored further in V-C.

For model inference, unlike model training, CPU energy may be significant, due to the need to constantly switch between CPU and GPU processing and the limited ability to batch multiple prompts. Since reading CPU energy via RAPL requires privileged access, and we did not have sudo access on the A100 machine, CPU energy data is only available for the RTX3070. As shown in Fig. 3, although all LLMs fit within the GPU's memory capacity, i.e., no model processing had to be done on the CPU, CPU energy consumption still accounted for approximately 16% of total energy usage, indicating a non-negligible contribution. This finding underscores

the importance of considering CPU energy consumption, even when the primary workload is handled by the GPU, as it can contribute significantly to overall energy costs.

Summary. Language models have varying energy footprints when performing diverse software development tasks. Even considering a codespecific model and two tasks that produce code, such as Code Generation and Bug Fixing, there may be a large difference in energy. Also, we have observed differences in energy usage of more than an order of magnitude between models performing the same task. The differences are not consistent across tasks. These trends could be observed for both machines. Finally, for inference, CPU energy can be non-negligible.

Implications. These findings highlight that the software development tasks that a model supports directly impact its energy use. Moreover, the differences in performance for different tasks can be large. Selecting models based on their expected tasks is crucial to reduce energy consumption.

B. When it comes to energy consumption and accuracy of LLMs in software development, it is not always a compromise.

Although energy consumption is an important quality attribute, the utility of a model is determined by its accuracy when performing inference. In this section, we investigate the relationship between the accuracy of the analyzed models in the 4 tasks and their energy footprint. Since the ideal scenario is one with low energy usage and high accuracy, we employed a Pareto front (or "Pareto frontier") analysis to determine whether a trade-off between these two objectives necessarily exists. The Pareto front identifies models that offer the best balance between minimizing energy usage and maximizing accuracy. By visualizing our results using this approach, we aim to highlight optimal solutions where improvements in one objective do not come at the expense of the other.

Figure 4(a) presents the results for Code Generation. The best results are the ones closer to the top left of the plot. It represents the overall lowest energy consumption and highest accuracy across all the models for this specific task. The Pareto front is indicated by the black dashed line. The figure shows that there are almost exclusively specialized coding models in the Pareto frontier, the only exception being llama3:8b. The other general-purpose models are dominated.

The results for phi3:3.8b are comparable to larger models in terms of accuracy but with a lower energy footprint. Models like Phi3-14b and Starcoder2-15b require 2.12 and 2.76 times as much energy, respectively, yet yield relatively small accuracy improvements of 4.27% and 3.05% over phi3:3.8b-q8's 59.75%. This diminishing return in accuracy relative to energy usage emphasizes that an increase in model size does not always correlate with proportional gains in energy efficiency. A model such as Granite-code:20b also illustrates this trend, requiring considerable energy for slight accuracy gains.

In contrast, in Bug Fixing (Figure 4(b)) and Docstring Generation (Figure 4(c)) general-purpose models exhibit competitive performance. The steep slope at the beginning of both Pareto fronts indicates that accuracy can be significantly improved with a relatively small increase in energy consumption emphasizing the trade-offs involved in model selection. Pareto fronts in Figure 4(a-c) show that small increases in energy consumption yield large gains in accuracy at first but then it reaches diminishing returns, where using more energy brings

only marginal improvements. A notable case for Docstring Generation is gemma:2b. The three models of this family are positioned near the ideal point. In particular, gemma:2b-fp16, a small model that could be run locally in a smartphone, is only surpassed in accuracy (70.12%) by gemma:7b-q4 (77.43%) and starcoder2:15b-q8 (75%), while these models consumed respectively 4.48 and 4.04 times more energy.

The Pareto frontier for Test Generation is relatively short. This shows that few solutions are close to the ideal point in terms of both energy consumption and accuracy for this task. There are only two models in the frontier: gemma:2b-q4 and codellama:7b-q4. The latter consumes 2.175 the energy of the former and has a 9% higher accuracy. Overall, codellama:7b-q4 exhibits the best accuracy across all the models in this task and is the 10th least energy-hungry model.

These plots also reinforce that there is variation in the energy footprint of the same model when performing different tasks. For instance, phi3:3.8b-fp16 is on the Pareto frontier for Code Generation, has reasonable performance for Test Generation, and performs poorly for Docstring Generation and Bug Fixing. Significant variation also exists when examining how multiple models perform the same task. For example, the third most energy-hungry model when generating tests on the A100, starcoder2:15b-fp16, consumed 13.98 times more energy than the least energy-hungry, gemma:2b-q4. Differences in energy footprint are not directly connected to differences in accuracy. The accuracy of gemma-2b-q4 for Test Generation was 75.6% vs. 71.34% for starcoder2:15b-fp16, even though the former is significantly smaller in the number of parameters and uses aggressive quantization. Even variants of the same model family can exhibit sizable differences in performing the same task. The model granite-code:20bfp16 when generating docstring consumed 7.8 times more energy than its smaller, quantized version, granite-code:3bq8. Complementarily, the two aforementioned variants of granite-code exhibited comparable accuracy when producing documentation, 50%, and 47.56% respectively.

Examining each model (data points with the same color) across different quantization levels (represented by different markers) shows moving quantized (q4 and q8) to full precision (fp16) yields only minimal accuracy gains at a substantial energy cost. In the plots, it is easy to see this by identifying the large number of squares and triangles that appear higher along the Y-axis. For all the tasks except for code generation, quantized models took the top spot in accuracy. Regardless of accuracy, our findings indicate that the smallest models with the most severe quantization level (Q4) consistently exhibited the lowest inference times across all four tasks on both hardware setups, with docstring generation being the fastest task. More details for both GPUs can be found in online appendices C and D [11].

These results highlight the importance of choosing the right model for the right task if it is going to be used intensively. This diversity of options allows practitioners to select models that align with specific requirements, optimizing for either energy efficiency, accuracy, or a combination of both. For

TABLE II: GPU A100 - Comparative results of inference in Code Generation (CG), Bug Fixing (BF), Docstring Generation (DG) and Test Generation(TG). C1 and C2 stand for statement and branch coverage of correct tests.

| Model name | Total energy (Wh) | | | | Accuracy% | | | | C1% | C2% | Efficiency (tokens/J) | | | |
|---------------------------|-------------------|--------|-------|--------|-----------|-------|-------|-------|-------|-------|-----------------------|------|------|------|
| | CG | BF | DG | TG | CG | BF | DG | TG | | | CG | BF | DG | TG |
| granite-code:20b-fp16* | 28.63 | 101.76 | 41.51 | 58.87 | 61.58 | 29.87 | 50.00 | 58.53 | 91.93 | 79.08 | 0.13 | 0.12 | 0.13 | 0.12 |
| granite-code:20b-q8 | 18.83 | 66.98 | 26.98 | 38.90 | 61.58 | 29.87 | 48.78 | 59.14 | 92.39 | 79.79 | 0.19 | 0.19 | 0.20 | 0.19 |
| granite-code:20b-q4 | 15.73 | 55.12 | 21.89 | 32.00 | 58.53 | 29.87 | 45.12 | 64.02 | 90.70 | 77.33 | 0.23 | 0.23 | 0.24 | 0.23 |
| starcoder2:15b-fp16* | 30.66 | 32.64 | 54.91 | 95.02 | 62.80 | 42.07 | 69.51 | 71.34 | 71.87 | 49.08 | 0.15 | 0.15 | 0.15 | 0.15 |
| starcoder2:15b-q8 | 19.84 | 21.87 | 34.33 | 66.89 | 63.41 | 42.07 | 75.00 | 70.73 | 69.39 | 45.54 | 0.24 | 0.22 | 0.24 | 0.24 |
| starcoder2:15b-q4 | 16.13 | 19.20 | 29.75 | 37.60 | 59.75 | 42.68 | 68.90 | 82.92 | 64.28 | 36.57 | 0.28 | 0.27 | 0.29 | 0.28 |
| phi3:14b-fp16* | 23.52 | 43.52 | 45.80 | 57.33 | 64.02 | 40.24 | 67.68 | 53.04 | 80.01 | 67.91 | 0.17 | 0.17 | 0.18 | 0.17 |
| phi3:14b-q8 | 15.58 | 27.80 | 29.83 | 39.58 | 61.58 | 41.46 | 68.90 | 51.82 | 79.21 | 66.54 | 0.27 | 0.27 | 0.28 | 0.27 |
| phi3:14b-q4 | 13.65 | 23.11 | 22.75 | 30.50 | 48.17 | 35.97 | 67.07 | 48.17 | 71.95 | 58.36 | 0.32 | 0.32 | 0.34 | 0.33 |
| codellama:13b-fp16* | 21.57 | 28.21 | 39.63 | 63.31 | 35.97 | 20.12 | 45.12 | 68.90 | 90.06 | 76.34 | 0.18 | 0.18 | 0.18 | 0.18 |
| codellama:13b-q8 | 14.31 | 19.47 | 25.25 | 39.14 | 40.24 | 18.29 | 45.12 | 70.12 | 90.81 | 76.37 | 0.28 | 0.27 | 0.29 | 0.28 |
| codellama:13b-q4 | 14.79 | 26.69 | 21.26 | 33.10 | 41.46 | 15.24 | 46.95 | 69.51 | 90.53 | 75.93 | 0.34 | 0.34 | 0.35 | 0.35 |
| llama2:13b-fp16 | 15.41 | 70.49 | 36.69 | 103.09 | 13.41 | 10.36 | 40.85 | 33.53 | 83.86 | 80.81 | 0.18 | 0.18 | 0.18 | 0.18 |
| llama2:13b-q8 | 10.61 | 45.93 | 23.55 | 66.36 | 14.02 | 9.75 | 40.85 | 33.53 | 83.13 | 78.76 | 0.27 | 0.28 | 0.29 | 0.28 |
| llama2:13b-q4 | 10.60 | 30.13 | 19.41 | 44.11 | 11.58 | 10.36 | 38.41 | 35.36 | 81.52 | 71.11 | 0.34 | 0.34 | 0.36 | 0.35 |
| granite-code:8b-fp16* | 12.78 | 48.33 | 19.43 | 51.58 | 42.68 | 20.12 | 58.53 | 60.97 | 70.66 | 42.65 | 0.26 | 0.26 | 0.26 | 0.26 |
| granite-code:8b-q8 | 8.47 | 31.30 | 12.52 | 33.59 | 42.68 | 20.73 | 57.92 | 57.92 | 70.67 | 42.57 | 0.40 | 0.40 | 0.41 | 0.41 |
| granite-code:8b-q4 | 7.28 | 26.95 | 10.71 | 27.68 | 38.41 | 18.29 | 59.14 | 65.85 | 70.50 | 41.19 | 0.46 | 0.46 | 0.48 | 0.47 |
| llama3:8b-fp16 | 10.86 | 15.94 | 17.72 | 27.99 | 54.87 | 40.24 | 50.00 | 31.70 | 84.06 | 80.66 | 0.27 | 0.27 | 0.28 | 0.28 |
| llama3:8b-q8 | 6.86 | 10.60 | 10.66 | 17.81 | 53.04 | 39.02 | 54.87 | 34.14 | 84.43 | 80.27 | 0.43 | 0.42 | 0.45 | 0.45 |
| llama3:8b-q4 | 6.43 | 9.64 | 10.13 | 18.17 | 53.65 | 40.24 | 52.43 | 26.21 | 81.60 | 80.40 | 0.50 | 0.48 | 0.52 | 0.50 |
| codegemma:7b-fp16* | 27.99 | 56.31 | 25.01 | 130.00 | 51.21 | 28.04 | 53.04 | 7.92 | 58.64 | 71.50 | 0.27 | 0.27 | 0.27 | 0.27 |
| codegemma:7b-q8 | 20.35 | 40.58 | 17.57 | 91.39 | 53.04 | 29.26 | 53.65 | 10.36 | 61.27 | 70.12 | 0.37 | 0.36 | 0.38 | 0.37 |
| codegemma:7b-q4 | 18.80 | 29.82 | 14.67 | 69.68 | 48.78 | 28.04 | 54.26 | 15.24 | 61.24 | 75.84 | 0.47 | 0.47 | 0.49 | 0.47 |
| codellama:7b-fp16* | 13.29 | 32.67 | 20.27 | 25.11 | 42.07 | 15.24 | 48.17 | 79.87 | 82.61 | 67.00 | 0.32 | 0.32 | 0.32 | 0.32 |
| codellama:7b-q8 | 8.78 | 21.39 | 12.63 | 15.68 | 40.24 | 16.46 | 44.51 | 81.70 | 83.94 | 66.95 | 0.50 | 0.49 | 0.51 | 0.50 |
| codellama:7b-q4 | 8.34 | 17.04 | 12.26 | 14.79 | 40.24 | 18.90 | 43.29 | 84.75 | 81.18 | 62.05 | 0.57 | 0.56 | 0.59 | 0.56 |
| deepseek-llm:7b-fp16 | 15.32 | 32.29 | 24.42 | 26.59 | 28.65 | 14.02 | 61.58 | 45.12 | 77.27 | 63.71 | 0.33 | 0.33 | 0.33 | 0.33 |
| deepseek-llm:7b-q8 | 9.95 | 21.62 | 16.21 | 16.95 | 28.65 | 15.85 | 60.97 | 40.85 | 76.61 | 63.75 | 0.51 | 0.50 | 0.52 | 0.51 |
| deepseek-llm:7b-q4 | 10.10 | 19.25 | 13.25 | 19.19 | 23.17 | 10.36 | 62.19 | 30.48 | 72.09 | 63.89 | 0.57 | 0.57 | 0.59 | 0.57 |
| gemma:7b-fp16 | 39.15 | 61.94 | 37.25 | 59.24 | 23.17 | 8.53 | 73.17 | 24.39 | 79.83 | 83.49 | 0.27 | 0.27 | 0.27 | 0.27 |
| gemma:7b-q8 | 29.24 | 45.83 | 27.97 | 43.47 | 26.82 | 8.53 | 70.12 | 21.95 | 79.36 | 82.92 | 0.37 | 0.37 | 0.37 | 0.37 |
| gemma:7b-q4 | 22.28 | 38.04 | 22.57 | 33.75 | 24.39 | 6.70 | 77.43 | 23.17 | 81.62 | 82.50 | 0.47 | 0.45 | 0.47 | 0.46 |
| llama2:7b-fp16 | 9.21 | 25.95 | 21.33 | 67.20 | 5.48 | 6.70 | 35.36 | 10.36 | 69.92 | 73.85 | 0.32 | 0.32 | 0.32 | 0.32 |
| llama2:7b-q8 | 6.07 | 16.65 | 13.44 | 43.71 | 6.09 | 6.09 | 40.85 | 12.80 | 72.10 | 75.31 | 0.49 | 0.49 | 0.52 | 0.50 |
| llama2:7b-q4 | 6.27 | 16.39 | 11.29 | 32.01 | 6.70 | 4.87 | 37.19 | 28.04 | 74.60 | 68.10 | 0.55 | 0.56 | 0.58 | 0.57 |
| mistral:7b-fp16 | 14.46 | 41.70 | 20.47 | 68.86 | 7.31 | 27.43 | 51.21 | 31.70 | 72.87 | 67.01 | 0.30 | 0.30 | 0.31 | 0.30 |
| mistral:7b-q8 | 9.56 | 27.09 | 13.33 | 44.14 | 4.87 | 24.39 | 51.82 | 29.26 | 71.22 | 68.87 | 0.48 | 0.47 | 0.48 | 0.47 |
| mistral:7b-q4 | 8.28 | 25.45 | 11.46 | 38.95 | 14.63 | 22.56 | 51.82 | 22.56 | 60.90 | 64.95 | 0.54 | 0.53 | 0.56 | 0.55 |
| deepseek-coder:6.7b-fp16 | 17.77 | 48.32 | 23.69 | 35.76 | 52.43 | 31.09 | 60.95 | 61.58 | 71.92 | 58.83 | 0.32 | 0.32 | 0.32 | 0.32 |
| deepseek-coder:6.7b-q8 | 12.05 | 33.14 | 15.40 | 22.25 | 54.26 | 31.70 | 68.90 | 58.53 | 74.67 | 60.71 | 0.50 | 0.50 | 0.52 | 0.50 |
| deepseek-coder:6.7b-q4 | 9.09 | 29.21 | 13.96 | 21.22 | 52.43 | 35.36 | 67.68 | 57.31 | 77.58 | 65.09 | 0.57 | 0.56 | 0.59 | 0.57 |
| phi3:3.8b-fp16 | 11.08 | 21.43 | 18.35 | 12.94 | 59.75 | 25.00 | 59.75 | 65.85 | 74.82 | 54.19 | 0.56 | 0.54 | 0.56 | 0.56 |
| phi3:3.8b-q8 | 8.16 | 16.05 | 13.07 | 9.18 | 58.53 | 19.50 | 56.70 | 64.63 | 76.15 | 55.44 | 0.75 | 0.73 | 0.77 | 0.74 |
| phi3:3.8b-q4 | 7.44 | 15.09 | 10.62 | 10.78 | 50.00 | 15.24 | 59.14 | 53.04 | 82.06 | 61.77 | 0.90 | 0.86 | 0.93 | 0.89 |
| granite-code:3b-fp16" | 6.80 | 22.35 | 7.22 | 24.46 | 45.12 | 20.73 | 47.56 | 76.21 | 69.54 | 39.12 | 0.57 | 0.55 | 0.58 | 0.56 |
| granite-code:3b-q8 | 5.29 | 16.71 | 5.27 | 17.58 | 45.12 | 20.73 | 47.56 | 78.65 | 69.17 | 38.97 | 0.75 | 0.75 | 0.78 | 0.76 |
| granite-code:3b-q4 | 4.27 | 14.28 | 3.96 | 15.43 | 41.46 | 14.63 | 44.51 | 71.34 | 70.55 | 42.38 | 0.91 | 0.89 | 0.94 | 0.90 |
| gemma:2b-fp16 | 9.87 | 8.56 | 8.50 | 10.85 | 18.29 | 17.07 | 70.12 | 65.24 | 80.77 | 63.10 | 0.80 | 0.80 | 0.80 | 0.80 |
| gemma:2b-q8 | 6.92 | 6.34 | 5.87 | 7.94 | 17.68 | 15.85 | 66.46 | 67.07 | 79.68 | 59.81 | 1.13 | 1.09 | 1.13 | 1.12 |
| gemma:2b-q4 | 5.76 | 4.86 | 4.84 | 6.80 | 20.73 | 16.46 | 67.68 | 75.60 | 79.65 | 61.22 | 1.28 | 1.25 | 1.30 | 1.28 |
| deepseek-coder:1.3b-fp16* | 9.23 | 17.03 | 5.08 | 12.35 | 6.70 | 6.09 | 42.07 | 23.17 | 70.35 | 48.24 | 1.47 | 1.41 | 1.55 | 1.44 |
| deepseek-coder:1.3b-q8 | 6.96 | 13.59 | 3.74 | 10.16 | 4.87 | 10.97 | 42.07 | 29.26 | 75.21 | 51.77 | 1.88 | 1.79 | 2.00 | 1.81 |
| deepseek-coder:1.3b-q4 | 5.89 | 10.73 | 2.79 | 7.57 | 3.65 | 5.48 | 40.24 | 28.65 | 72.29 | 50.06 | 2.29 | 2.14 | 2.39 | 2.19 |

^{*} Code-specific model families.

example, in contexts where high accuracy is essential but energy costs are a concern phi3:3.8b or gemma:2b could be prioritized. Conversely, if energy is less of a constraint and marginal accuracy improvements are critical, larger models could be considered. Finally, code-specific models outperforming general models in accuracy solely in code generation, without any general model appearing in the top 10 in terms of accuracy, suggests that the training data for these models may be more concentrated on code synthesis, while the data available for other tasks may be less extensive or specialized.

Summary. Larger models often have a much greater energy footprint while usually performing close to or even being outperformed by smaller models in terms of accuracy. We observed that small increases in energy consumption result in substantial accuracy improvements, but then a point of diminishing returns is reached, emphasizing that an increase in model size does not always correlate with proportional gains in accuracy. Additionally, quantized models sometimes exhibit higher accuracy than their full-precision counterparts while having much lower model sizes.

Implications. The results show that not all models follow a strict trade-off pattern between accuracy and energy use when considering different software development tasks. In some cases, a model that consumes (relatively) little energy also exhibits a high accuracy, and it is not necessary to prioritize one attribute to the detriment of the other, i.e., it is not necessary to find a compromise solution.

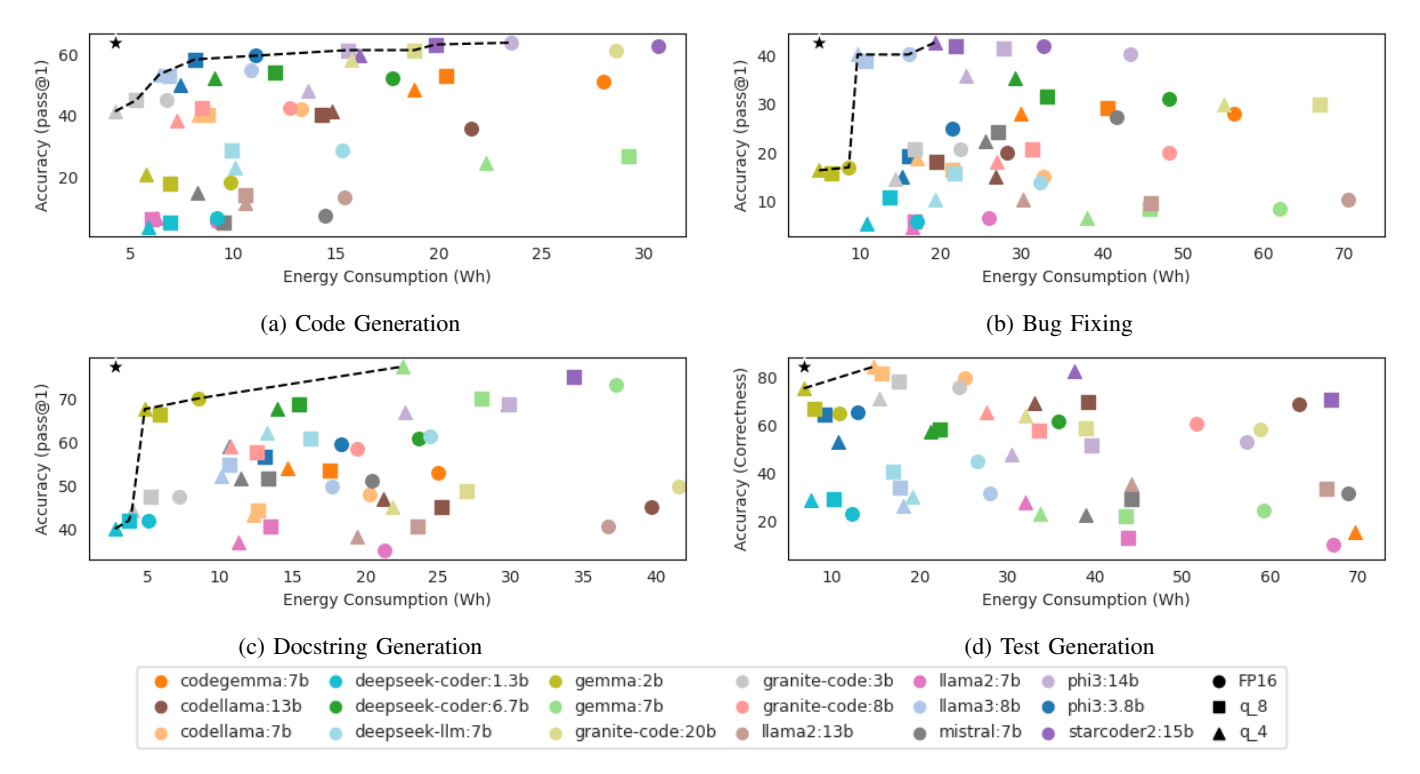


Fig. 4: Relation between accuracy and total energy for each task on GPU A100. Black dashed line indicates the Pareto frontier. The ★ marker denotes the ideal point. (Data points exceeding the y-axis limit are not displayed.)

C. Characteristics of a model's architecture have a strong correlation with its efficiency measured in the number of output tokens per joule.

Fig. 5 shows a correlation matrix between six characteristics of a model's architecture and five performance metrics. The numbers in the cells indicate the Spearman correlation coefficient between two variables, e.g., -0.42 is the correlation between Bit Width and Tokens per Joule. The matrix only presents coefficients for which the p-value is statistically significant, e.g., the correlation between Parameter Count and Accuracy is not statistically significant. All the values in the correlation matrix in Figure 5 are based on an adjusted alpha value. To control the family-wise error rate, we applied the Bonferroni correction by dividing the default alpha value (0.05) by the number of conducted tests (30). All the numbers in the matrix have a p-value lower than 0.0016.

This figure shows that parameter count does not have a statistically significant correlation with model accuracy. This result underscores the findings of Section V-B, that larger models do not necessarily produce more accurate results than smaller ones. In addition, parameter count exhibits a very strong negative correlation with the number of output tokens per joule efficiency metric. For this metric, a high value is better, as it quantifies the efficiency of a model, instead of just its resource usage. The strong negative correlation points out that the larger the number of parameters of a model the more energy it requires per output token. In addition, the metric tokens per joule is strongly correlated with every analyzed

model characteristic, except for bit width, with which it is moderately correlated. The "Efficiency (tokens/J)" column of Table II also indicates that tokens per joule may be a useful metric to analyze model performance across different software development tasks. Despite the observed variation in overall energy consumption across different tasks, the table shows a small variation in the value of the metric, per model, regardless of task. Parameter count also has a moderate (total time and GPU memory) to strong (total energy) positive correlation with the remaining performance metrics. The remaining model characteristics exhibit statistically significant correlations with the performance metrics (except for accuracy) ranging from weak to strong. These findings confirm that larger models tend to be slower, consume more energy, and require more memory.

The strong positive correlation between memory usage and bit width confirms that lower-precision models require less memory bandwidth and storage, reducing the energy required for data transfer and memory access. Results in Table II indicate that fp16 variants have lower efficiency in tokens/J than 8- or 4-bit variants. The 4-bit variant of each model exhibited the highest performance in tokens/J for all tasks and the lowest energy usage in 212 out of the 216 analyzed cases.

As shown in Figure. 5, Energy consumption is positively correlated with key hyperparameters, such as the number of attention heads, feed-forward network dimension, number of transformer blocks, embedding size, and overall model size. These hyperparameters vary across models, influencing their energy usage. We also observe that energy consumption is

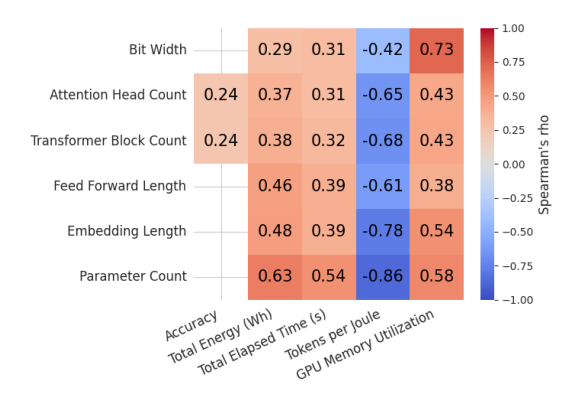


Fig. 5: Spearman's correlation matrix for all models across all tasks on GPU A100 (p-value < 0.0016)

moderately correlated with the token count in the generated output (statistic = 0.58, p-value = 3.79e-21). In all the analyzed cases inference time and overall energy usage have an almost perfect correlation (statistic=0.98, pvalue=7.76e-161).

Summary. The performance metrics, except for accuracy, are correlated with the architectural characteristics of the models. Furthermore, among these metrics, tokens/J exhibits the highest correlation coefficients, particularly with the parameter count. In addition, the consistent tokens/J observed across all four tasks highlights it as an effective metric for evaluating the efficiency of the models.

Implications. LLM architecture, together with the expected size of the output produced for a given task, can help us estimate a model's energy efficiency when performing software development tasks. Model size is not a reliable predictor for a model's accuracy in software development tasks.

D. Coding models are not particularly good for tasks other than generating code, if energy consumption matters.

According to our results, there is no relationship between a model's energy consumption and whether it is code-specific or general-purpose. Our analysis reveals that when we only consider accuracy, coding-specific LLMs on average outperform general-purpose LLMs in 3 out of the 4 tasks evaluated. Coding models achieve higher accuracy compared to general ones for Code Generation, Bug Fixing, and Test Generation, with mean accuracies of 46.45% vs. 21.77%, 24.83% vs. 16.92%, and 57.61% vs. 34.43%, respectively. For Docstring Generation, general models slightly outperform coding models, with accuracies of 55.02% and 54.78%, respectively.

A careful examination of the results paints a more nuanced picture. For Bug Fixing, the accuracy of the models was generally low; the highest value reached only 42.68%. When we factor in energy consumption, most models in the Pareto frontier (Figure 4(c)) are non-coding models (gemma:2b and llama3:8b families), the exception being starcoder2:15b-q4, the model with the highest accuracy in this task. The accuracy of llama3:8b-q4 was 2.4% lower than the best while consuming only 50% of the energy. Moreover, for Test Generation (Figure 4(d)), there are only two models in the Pareto frontier, one of them gemma:2b-q4, a non-coding model. Furthermore, there is a small cluster of models near the Pareto frontier and the others consume much more energy, have much

lower accuracy, or both. For Docstring Generation, the points in the Pareto frontier are a mix of coding and non-coding models. Code Generation is the only task where there are almost exclusively coding models along the Pareto frontier (Figure 4(a)), the exception being llama3:8b-q4.

Summary. Coding models exhibited better mean accuracy than noncoding models, although the results were inconclusive for energy efficiency. However, for Docstring Generation and Test Generation some non-coding models exhibited both high accuracy and low energy consumption. No model fared particularly when in Bug Fixing.

Implications. "Coding"-specific models can be more accurately described as "code generation" models. Our findings suggest that fine-tuning models for other tasks, such as documentation generation and bug fixing, is a potential research avenue to improve accuracy and energy efficiency.

VI. THREATS TO VALIDITY

A potential threat to *internal validity* in this study relates to the use of prompt templates. For the sake of fair energy comparison, we used the same prompts across all models within each task, without tailoring them to individual model capabilities. This uniform approach may have resulted in differences in accuracy compared to results reported in the literature. Moreover, a few models experienced incomplete cases when using the Ollama API, where packets received were not fully completed. Although we adjusted the token limit to mitigate this issue, it persisted and may have impacted the accuracy of certain models, thus affecting internal consistency. Additionally, the process of extracting generated code from the LLMs' responses can also introduce a potential threat to internal validity. A few models did not include clear starting and ending markers for code sections, making it difficult to accurately detect the intended answer using regular expressions. To address this, we first employed a regular expression approach and subsequently used an open-access powerful LLM (gpt4o-mini) to extract the code from natural language explanations. Despite these efforts, this process may still negatively impact the accuracy evaluation of some models.

Another potential limitation is that our evaluation is based solely on the HumanEvalPack dataset, which includes only basic functions and may not fully represent real-world software development tasks. This constraint reduces the generalizability of our findings to more complex or varied coding scenarios, potentially impacting the *external validity* of this study. Furthermore, we only evaluated models using the Python programming language, which limits the diversity of real-world programming tasks covered. General models may benefit from Python's high-level syntax, especially when generating docstrings, due to the relative ease of understanding Python functions. Including additional programming languages would improve the generalizability of the results.

Finally, the study lacks a sufficient number of comparable pairs of general-purpose models and their code-optimized counterparts. This shortcoming limits the strength of our conclusions regarding energy consumption differences between general and specialized LLMs. We mitigated this threat by analyzing a wide range of models in terms of sizes, companies

that produced them, and whether they are coding-specific or non-coding-specific.

VII. CONCLUSION

Our findings indicate that larger models often have higher energy consumption without proportional accuracy gains and can sometimes be outperformed by smaller models, suggesting that model size alone is not a reliable predictor of accuracy. We found that a model's energy usage varies significantly across software development tasks, highlighting the importance of selecting models fine-tuned to specific applications to manage energy consumption effectively and maximize efficiency. Although energy usage varies across tasks, the energy consumption per generated token remains consistent for a given model. Moreover, the strong correlation between total energy consumption and architectural characteristics, particularly parameter count, suggests that an LLM's architecture can serve as a useful indicator of its energy efficiency, given that the average size of the outputs can be anticipated. Finally, considering both energy and accuracy, coding-specific models outperformed general models only in code generation tasks. This indicates that fine-tuning these models for other tasks, such as documentation generation and bug fixing, could be a promising research direction to enhance their accuracy and energy efficiency.

REFERENCES

- C. Ebert and P. Louridas, "Generative AI for software practitioners," *IEEE Softw.*, vol. 40, no. 4, pp. 30–38, 2023. [Online]. Available: https://doi.org/10.1109/MS.2023.3265877
- [2] Microsoft Corporation, "AI at Work Is Here—Now Comes the Hard Part," 2024, accessed: 2024-11-05. [Online]. Available: https://www.microsoft.com/en-us/worklab/work-trend-index/ai-atwork-is-here-now-comes-the-hard-part
- [3] Stack Overflow, "Developers get by with a little help from ai: Stack overflow knows code - assistant pulse survey results," 2024, accessed: 2024-11-08. [Online]. Available: https: //stackoverflow.blog/2024/05/29/developers-get-by-with-a-little-helpfrom-ai-stack-overflow-knows-code-assistant-pulse-survey-results/
- [4] GitHub, "Research: Quantifying github copilot's impact in the enterprise with accenture," 2024, accessed: 2024-11-08. [Online]. Available: https://github.blog/news-insights/research/research-quantifying-github-copilots-impact-in-the-enterprise-with-accenture/
- [5] E. Strubell, A. Ganesh, and A. McCallum, "Energy and policy considerations for deep learning in NLP," CoRR, vol. abs/1906.02243, 2019.
- [6] A. Lacoste, A. Luccioni, V. Schmidt, and T. Dandres, "Quantifying the carbon emissions of machine learning," *CoRR*, vol. abs/1910.09700, 2019.
- [7] A. S. Luccioni, S. Viguier, and A. Ligozat, "Estimating the carbon footprint of bloom, a 176b parameter language model," *CoRR*, vol. abs/2211.02001, 2022.
- [8] D. A. Patterson, J. Gonzalez, U. Hölzle, Q. V. Le, C. Liang, L. Munguia, D. Rothchild, D. R. So, M. Texier, and J. Dean, "The carbon footprint of machine learning training will plateau, then shrink," *Computer*, vol. 55, no. 7, pp. 18–28, 2022.
- [9] Z. Zheng, K. Ning, Y. Wang, J. Zhang, D. Zheng, M. Ye, and J. Chen, "A survey of large language models for code: Evolution, benchmarking, and future trends," *CoRR*, vol. abs/2311.10372, 2023.
- [10] J. Jiang, F. Wang, J. Shen, S. Kim, and S. Kim, "A survey on large language models for code generation," *CoRR*, vol. abs/2406.00515, 2024.
- [11] Anonymous, "Replication package," November 2024, accessed: 2024-11-09. [Online]. Available: https://doi.org/10.5281/zenodo.14064267

- [12] A. Vaswani, N. Shazeer, N. Parmar, J. Uszkoreit, L. Jones, A. N. Gomez, L. Kaiser, and I. Polosukhin, "Attention is all you need," in Advances in Neural Information Processing Systems 30: Annual Conference on Neural Information Processing Systems 2017, December 4-9, 2017, Long Beach, CA, USA, 2017, pp. 5998–6008.
- [13] Z. Wang, Z. Chu, T. V. Doan, S. Ni, M. Yang, and W. Zhang, "History, development, and principles of large language models: an introductory survey," AI and Ethics, pp. 1–17, 2024.
- [14] R. Jin, J. Du, W. Huang, W. Liu, J. Luan, B. Wang, and D. Xiong, "A comprehensive evaluation of quantization strategies for large language models," in *Findings of the Association for Computational Linguistics*, ACL 2024, Bangkok, Thailand and virtual meeting, August 11-16, 2024. Association for Computational Linguistics, 2024, pp. 12186–12215.
- [15] R. Gong, Y. Ding, Z. Wang, C. Lv, X. Zheng, J. Du, H. Qin, J. Guo, M. Magno, and X. Liu, "A survey of low-bit large language models: Basics, systems, and algorithms," *CoRR*, vol. abs/2409.16694, 2024.
- [16] S. Rajput and T. Sharma, "Benchmarking emerging deep learning quantization methods for energy efficiency," in 21st IEEE International Conference on Software Architecture, ICSA 2024 - Companion, Hyderabad, India, June 4-8, 2024. IEEE, 2024, pp. 238–242.
- [17] C. Watson, N. Cooper, D. Nader-Palacio, K. Moran, and D. Poshyvanyk, "A systematic literature review on the use of deep learning in software engineering research," ACM Trans. Softw. Eng. Methodol., vol. 31, no. 2, pp. 32:1–32:58, 2022.
- [18] M. Pradel and K. Sen, "Deepbugs: A learning approach to name-based bug detection," *Proceedings of the ACM on Programming Languages*, vol. 2, no. OOPSLA, pp. 1–25, 2018.
- [19] Q. Chen, C. Yu, R. Liu, C. Zhang, Y. Wang, K. Wang, T. Su, and L. Wang, "Evaluating the effectiveness of deep learning models for foundational program analysis tasks," *Proceedings of the ACM on Programming Languages*, vol. 8, no. OOPSLA1, pp. 500–528, 2024.
- [20] N. Muennighoff, Q. Liu, A. Zebaze, Q. Zheng, B. Hui, T. Y. Zhuo, S. Singh, X. Tang, L. von Werra, and S. Longpre, "Octopack: Instruction tuning code large language models," *CoRR*, vol. abs/2308.07124, 2023.
- [21] M. Chen, J. Tworek, H. Jun, Q. Yuan, H. P. de Oliveira Pinto, J. Kaplan, H. Edwards *et al.*, "Evaluating large language models trained on code," *CoRR*, vol. abs/2107.03374, 2021.
- [22] B. Rozière, J. Gehring, F. Gloeckle, S. Sootla, I. Gat, X. E. Tan, Y. Adi, J. Liu, T. Remez, J. Rapin, A. Kozhevnikov, I. Evtimov, J. Bitton, M. Bhatt, C. Canton-Ferrer, A. Grattafiori, W. Xiong, A. Défossez, J. Copet, F. Azhar, H. Touvron, L. Martin, N. Usunier, T. Scialom, and G. Synnaeve, "Code llama: Open foundation models for code," CoRR, vol. abs/2308.12950, 2023.
- [23] R. Li, L. B. Allal, Y. Zi, N. Muennighoff, D. Kocetkov, C. Mou, M. Marone, C. Akiki, J. Li, J. Chim et al., "Starcoder: may the source be with you!" *Trans. Mach. Learn. Res.*, vol. 2023, 2023.
- [24] J. Zhang, J. P. Cambronero, S. Gulwani, V. Le, R. Piskac, G. Soares, and G. Verbruggen, "Pydex: Repairing bugs in introductory python assignments using llms," *Proc. ACM Program. Lang.*, vol. 8, no. OOPSLA1, pp. 1100–1124, 2024.
- [25] L. F. W. Anthony, B. Kanding, and R. Selvan, "Carbontracker: Tracking and predicting the carbon footprint of training deep learning models," *CoRR*, vol. abs/2007.03051, 2020.
- [26] D. Li, X. Chen, M. Becchi, and Z. Zong, "Evaluating the energy efficiency of deep convolutional neural networks on cpus and gpus," in 2016 IEEE International Conferences on Big Data and Cloud Computing (BDCloud), Social Computing and Networking (SocialCom), Sustainable Computing and Communications (SustainCom), BDCloud-SocialCom-SustainCom 2016, Atlanta, GA, USA, October 8-10, 2016. IEEE Computer Society, 2016, pp. 477–484.
- [27] T. Yarally, L. Cruz, D. Feitosa, J. Sallou, and A. van Deursen, "Uncovering energy-efficient practices in deep learning training: Preliminary steps towards green AI," in 2nd IEEE/ACM International Conference on AI Engineering Software Engineering for AI, CAIN 2023, Melbourne, Australia, May 15-16, 2023. IEEE, 2023, pp. 25–36.
- [28] N. C. Thompson, K. H. Greenewald, K. Lee, and G. F. Manso, "The computational limits of deep learning," *CoRR*, vol. abs/2007.05558, 2020
- [29] J. McDonald, B. Li, N. C. Frey, D. Tiwari, V. Gadepally, and S. Samsi, "Great power, great responsibility: Recommendations for reducing energy for training language models," in *Findings of the Association for Computational Linguistics: NAACL 2022, Seattle, WA, United States, July 10-15, 2022.* Association for Computational Linguistics, 2022, pp. 1962–1970.

- [30] R. Desislavov, F. Martínez-Plumed, and J. Hernández-Orallo, "Compute and energy consumption trends in deep learning inference," *CoRR*, vol. abs/2109.05472, 2021.
- [31] S. Samsi, D. Zhao, J. McDonald, B. Li, A. Michaleas, M. Jones, W. Bergeron, J. Kepner, D. Tiwari, and V. Gadepally, "From words to watts: Benchmarking the energy costs of large language model inference," in *IEEE High Performance Extreme Computing Conference*, *HPEC 2023, Boston, MA, USA, September 25-29, 2023*. IEEE, 2023, pp. 1–9.
- [32] S. Luccioni, Y. Jernite, and E. Strubell, "Power hungry processing: Watts driving the cost of AI deployment?" in *The 2024 ACM Conference on Fairness, Accountability, and Transparency, FAccT 2024, Rio de Janeiro, Brazil, June 3-6, 2024.* ACM, 2024, pp. 85–99.
 [33] L. Tuggener, P. Sager, Y. Taoudi-Benchekroun, B. F. Grewe, and
- [33] L. Tuggener, P. Sager, Y. Taoudi-Benchekroun, B. F. Grewe, and T. Stadelmann, "So you want your private LLM at home? A survey and benchmark of methods for efficient gpts," in 11th IEEE Swiss Conference on Data Science, SDS 2024, Zurich, Switzerland, May 30-31, 2024. IEEE, 2024, pp. 205–212.
- [34] Hugging Face, "Hugging Face: The AI Community Building the Future," 2024, accessed: 2024-11-05. [Online]. Available: https://huggingface.co/
- [35] Ollama, "Ollama Model Library," 2024, accessed: 2024-11-05. [Online]. Available: https://ollama.com/library
- [36] G. Gerganov, "GGUF Format Documentation," 2023, accessed: 2024-11-05. [Online]. Available: https://github.com/ggerganov/ggml/blob/master/docs/gguf.md
- [37] Georgi Gerganov, "llama.cpp: A C++ Implementation of LLaMA Model," 2023, accessed: 2024-11-05. [Online]. Available: https://github.com/ggerganov/llama.cpp
- [38] EvalPlus, "EvalPlus Leaderboard," 2023, accessed: 2024-11-05. [Online]. Available: https://evalplus.github.io/leaderboard.html
- [39] J. Liu, C. S. Xia, Y. Wang, and L. Zhang, "Is your code generated by chatgpt really correct? rigorous evaluation of large language models for code generation," in Advances in Neural Information Processing Systems 36: Annual Conference on Neural Information Processing Systems 2023, NeurIPS 2023, New Orleans, LA, USA, December 10 - 16, 2023, 2023.
- [40] LangChain, "How to use local llms," 2024, accessed: 2024-07-15. [Online]. Available: https://python.langchain.com/v0.2/docs/how_to/local llms/#inference
- [41] N. Alizadeh and F. Castor, "Green AI: a preliminary empirical study on energy consumption in DL models across different runtime infrastructures," in *Proceedings of the IEEE/ACM 3rd International Conference* on AI Engineering - Software Engineering for AI, CAIN 2024, Lisbon, Portugal, April 14-15, 2024. ACM, 2024, pp. 134–139.
- [42] M. F. Argerich and M. Patiño-Martínez, "Measuring and improving the energy efficiency of large language models inference," *IEEE Access*, vol. 12, pp. 80 194–80 207, 2024.
- [43] F. Castor, "Estimating the energy footprint of software systems: a primer," *CoRR*, vol. abs/2407.11611, 2024.
- [44] NVIDIA Corporation, "NVIDIA Management Library (NVML)," 2024, https://developer.nvidia.com/management-library-nvml. Last accessed August 20th, 2024.
- [45] PyPI Contributors, "pynvml: Python bindings for NVML," 2024, accessed: 2024-11-06. [Online]. Available: https://pypi.org/project/ pvnvml/
- [46] K. N. Khan, M. Hirki, T. Niemi, J. K. Nurminen, and Z. Ou, "RAPL in action: Experiences in using RAPL for power measurements," ACM Trans. Model. Perform. Evaluation Comput. Syst., vol. 3, no. 2, pp. 9:1– 9:26, 2018.
- [47] PyPI Contributors, "pyRAPL: Python library for measuring energy consumption with RAPL," 2024, accessed: 2024-11-06. [Online]. Available: https://pypi.org/project/pyRAPL/
- [48] Intel Corporation, "Running Average Power Limit (RAPL) Energy Reporting," 2024, accessed: 2024-11-05. [Online]. Available: https://www.intel.com/content/www/us/en/developer/articles/technical/ software-security-guidance/advisory-guidance/running-average-powerlimit-energy-reporting.html
- [49] NVIDIA Corporation, "NVIDIA System Management Interface (nvidia-smi)," 2024, accessed: 2024-11-06. [Online]. Available: https://developer.nvidia.com/system-management-interface
- [50] A. Lozhkov, R. Li, L. B. Allal, F. Cassano, J. Lamy-Poirier, N. Tazi, A. Tang, D. Pykhtar, J. Liu, Y. Wei et al., "Starcoder 2 and the stack v2: The next generation," CoRR, vol. abs/2402.19173, 2024.
- [51] M. Du, A. T. Luu, B. Ji, and S. Ng, "Mercury: An efficiency benchmark for LLM code synthesis," *CoRR*, vol. abs/2402.07844, 2024.

- [52] Y. Wei, Z. Wang, J. Liu, Y. Ding, and L. Zhang, "Magicoder: Empowering code generation with oss-instruct," in Forty-first International Conference on Machine Learning, ICML 2024, Vienna, Austria, July 21-27, 2024. OpenReview.net, 2024.
- [53] R. Taori, I. Gulrajani, T. Zhang, Y. Dubois, X. Li, C. Guestrin, P. Liang, and T. B. Hashimoto, "Alpaca: A strong, replicable instructionfollowing model," *Stanford Center for Research on Foundation Models.* https://crfm. stanford. edu/2023/03/13/alpaca. html, vol. 3, no. 6, p. 7, 2023.
- [54] K. Li and Y. Yuan, "Large language models as test case generators: Performance evaluation and enhancement," CoRR, vol. abs/2404.13340, 2024
- [55] N. Batchelder, "Coverage.py: The code coverage tool for Python." [Online]. Available: https://github.com/nedbat/coveragepy